



MODAL PARAMETERS FITTING OF COMPOSITE FLAT PLATES FOR AEROELASTIC ANALYSIS

Hermann Luís Lebkuchen

Universidade Federal de Santa Catarina - UFSC - Joinville, SC, Brazil

Adolfo Gomes Marto

Instituto de Aeronáutica e Espaço - IAE - São José dos Campos, SP, Brazil

Carlos Eduardo de Souza

Aeroest Eng. & Tecnologia - Porto Alegre, RS, Brazil

Abstract. In this work a parameters fitting methodology is applied to laminated composite plates used in aeroelastic wing models. Experimental modal analysis results are used as reference values for correlation maximization, compared to numerical values obtained from finite element simulation. An optimization process is used, where the objective function includes information on the experimental and numerical natural frequencies. Numerical studies with different FEM discretization models of an isotropic cantilever beam are adjusted. Fitting methodology is extended to orthotropic models where shear modulus and the spanwise and chordwise elasticity moduli of laminated composite plates are fitted. The modal assurance criterion is used to verify that the mode shapes are correctly correlated. A code in Matlab™ is developed, using MSC Nastran™ as the finite element solver for numerical modal analyses. The methodology is successfully applied to the parameters fitting of unidirectional carbon fiber plates, supporting complete aeroelastic tests.

Keywords: modal parameters fitting, FEM, aeroelastic wing models, composite materials, .

1. INTRODUCTION

In this work, structural parameter fitting techniques applied to orthotropic plates used in aeroelastic tests are studied. The goal is to find by successive iterations the structural parameters of finite element method (FEM) model that corresponds to the physical model. The mean idea consists in applying a cost function based on residue between the numerical and experimental eigenvalues and eigenvectors.

This methodology is useful for dealing with aeroelastic dynamic systems where FEM is used as a numeric tool to represent the system dynamics. Since the numeric model differs from physical, the fitting methodology is employed to obtain adequate parameters, based on results from experimental modal analysis (EMA) or operational modal analyses (OMA) are used to obtain natural modes frequencies and shapes of the physical model.

The mathematical background of the present work is similar to that employed by Infantes (2000) and Göge (2003). The parameters updating results of an least squares minimization of the residue between reference (experimental) and adjusting (numerical) data. Modal assurance criterion (MAC) is applied to verify the correlation between actual and numerical modes (Allemang, 2003).

To automate the fitting process, the computational tools MSC Nastran™ and Matlab™ are coupled to solve the modal problem and to implement iterative correction. The ability of fitting orthotropic numerical models is an advantage in view of several applications on aeronautical and aerospace field as well as wind turbines, where low weight and excellent mechanical properties are essential to increase performance.

To validate the methodology, an isotropic aluminum cantilever beam is studied, as in Infantes (2000) . The elasticity modulus and equivalent translational and torsional springs at root are fitted. Models with different number of points are used to verify the interpolation process. To achieve the goals of dealing with composite plates, the methodology is also applied to a flat plate made of orthotropic material, where shear modulus and the spanwise and chordwise elasticity moduli are fitted. To complement the work, a composite flat plate used in aeroelastic tests performed by de Souza *et al.* (2013) is analyzed. In that work, EMA and OMA methodologies were used to characterize the modal behavior of composite flat plates made of carbon fiber and epoxy for aeroelastic analyses purposes.

2. PARAMETERS FITTING METHODOLOGY

The process of parameters fitting methodology is to update the structural parameters, θ , of a numerical model until they correspond as close as physical model. Manual corrections are slower than a automated method. The high time exposure of the manual correction is a major drawback compared with computational iterative methods (Göge, 2003). Another problem in manual correction is when the model has more than one structural parameter to be predicted since the global dynamic behavior is affected by each parameter. Even though, the parameters fitting methodology allow multiple parameters fit in much less time. Following Infantes (2000), the mathematical method used is the least squares in order to

minimize the cost function, which is defined as:

$$J(\partial\theta) = \frac{1}{2}\epsilon^T\epsilon, \quad (1)$$

where the term ϵ is a residue between numerical and experimental data, given by:

$$\epsilon = \partial\mathbf{z}_m - \partial\bar{\mathbf{z}}, \quad (2)$$

Here, $\partial\mathbf{z}_m$ is a vector that contains the experimental data, arranged in the follow way:

$$\mathbf{z}_m = \{\lambda_1 \quad \lambda_2 \quad \dots \quad \lambda_p \quad \phi_1^T \quad \phi_2^T \quad \dots \quad \phi_p^T\}^T. \quad (3)$$

The term $\bar{\mathbf{z}}$ is a vector that contains the analytical data depending on the model parameters (Göge, 2003). The analytical vector is nonlinear, and a truncated Taylor series is used for linearization:

$$z(\theta_1, \theta_2, \theta_3, \dots, \theta_n) = \bar{z}(\bar{\theta}_1, \bar{\theta}_2, \bar{\theta}_3, \dots, \bar{\theta}_n) + \sum_{i=1}^n \frac{\partial z}{\partial \theta_i} (\theta_i - \bar{\theta}_i), \quad (4)$$

or, in a short representation,

$$\partial\bar{\mathbf{z}} = \left[\frac{\partial \mathbf{z}}{\partial \theta} \right] \partial\theta \longrightarrow \partial\bar{\mathbf{z}} = \mathbf{S}_j \partial\theta. \quad (5)$$

The terms in the above equation are: $\partial\theta = \theta - \theta_j$ represents the parameter variation, and \mathbf{S}_j is the sensitivity matrix. Inserting the residue, Eq. (2), in the cost function, Eq. (1), it is obtained:

$$J(\partial\theta) = \partial\mathbf{z}^T \partial\mathbf{z} - 2\partial\theta^T \mathbf{S}_j^T \partial\mathbf{z} + \partial\theta^T \mathbf{S}_j^T \mathbf{S}_j \partial\theta, \quad (6)$$

and applying the least square method on the above equation means to minimize J in relation to $\partial\theta$,

$$\nabla J(\partial\theta) = -\mathbf{S}_j^T \partial\mathbf{z} + \mathbf{S}_j^T \mathbf{S}_j \partial\theta = 0, \quad (7)$$

solving Eq. (7) to $\partial\theta$,

$$\partial\theta = [\mathbf{S}_j^T \mathbf{S}_j]^{-1} \mathbf{S}_j^T \partial\mathbf{z}. \quad (8)$$

By this formulation, the fitted parameters can be obtained by,

$$\theta_{j+1} = \theta_j + [\mathbf{S}_j^T \mathbf{S}_j]^{-1} \mathbf{S}_j^T (\mathbf{z}_m - \mathbf{z}_j). \quad (9)$$

The formulation for parameters fitting presented above does not consider weighting, hence all measured data is equally pondered (Infantes, 2000). In order to evaluate Eq. (9) the sensitivity matrix must be defined.

2.1 Sensitivities

Design sensitivity analysis (DSA) is a design tool for estimating effects of many interrelated design variables such as element properties and materials on the structural response (Lahey, 1983). The DSA is used to compute the values of the design sensitivity coefficients which are defined as the gradients of the design variables at the current design point, and the computation of these parameters are the major task of sensitivity development. Hence, structural sensitivity consists in changing the design variables in search for a better solution during the parameters fitting process (Jurado *et al.*, 2012). Sensitivity matrix contain eigenvalues, λ , and eigenvectors, ψ derivatives, and the size of S matrix vary with the number of structural parameters n and the number of natural modes, m . The sensitivity matrix is contains the partial derivatives of the eigenvectors and

$$\mathbf{S} = \begin{bmatrix} \frac{\partial \lambda}{\partial \theta_1} & \frac{\partial \lambda}{\partial \theta_2} & \dots & \frac{\partial \lambda_m}{\partial \theta_n} \\ \frac{\partial \psi}{\partial \theta_1} & \frac{\partial \psi}{\partial \theta_2} & \dots & \frac{\partial \psi_m}{\partial \theta_n} \end{bmatrix}. \quad (10)$$

Infantes (2000) used an analytical formulation to obtain sensitivities. In the present work, however, it was decided to use finite differences. Since MSC NastranTM is used to calculate the modes, there was no information on the mass and stiffness matrices. Because the models are small enough, the calculation of modes at each design point is not expensive, and can be afforded.

2.2 Model correlation

Working with parameter fitting methodology, data of experimental and numerical models have to be correlated. When the number of modes in a EMA are large, is not easy to correlate each one in FEM model by manual process. For this reason, the *modal assurance criterion* (MAC) is used to provide a measure of consistency, or in other words a degree of linearity, between estimates of a modal vector. This provides an additional confidence factor in the evaluation of a modal vector from different excitation locations or different modal parameter estimation algorithms.

Modal assurance criterion is defined as a scalar constant relating the degree of consistency between one modal and another reference modal vector (Allemang, 2003). MAC is defined as,

$$MAC_{ij} = \frac{|\psi_{m_i}^T \psi_{a_j}|^2}{(\psi_{m_i}^T \psi_{m_i})(\psi_{a_j}^T \psi_{a_j})}. \quad (11)$$

Good correlations between numerical and experimental models occur when the matrix mean diagonal is nearly 1. Terms nearly 0 represent non correlated modal shapes (Infantes, 2000). When terms out of the matrix mean diagonal are close 1 modal shapes between models have problems such as exchange or coupled modal shapes. Definitely MAC is a suitable way to check correlations, and is usually represented by a matrix or colored charts.

Here, it is necessary to have the modes represented in the same model, because vector need to be adequately sized. Interpolation of mode shapes is common process in aeroelastic analysis. In the present work, interpolation by use of splines is implemented to bring the reference mode shapes to the fitting model. The reader is referred to ZONA Technology (2007) for more details on the method.

3. CODE IMPLEMENTATION

The methodology described above is implemented in Matlab™, and uses MSC Nastran™ as the structural solver. The flowchart, given in Fig. 1 follows the one presented by Infantes (2000) and Carneiro (1993), but here the sensitivity is calculated in a much simpler way, as described in section 2.1.

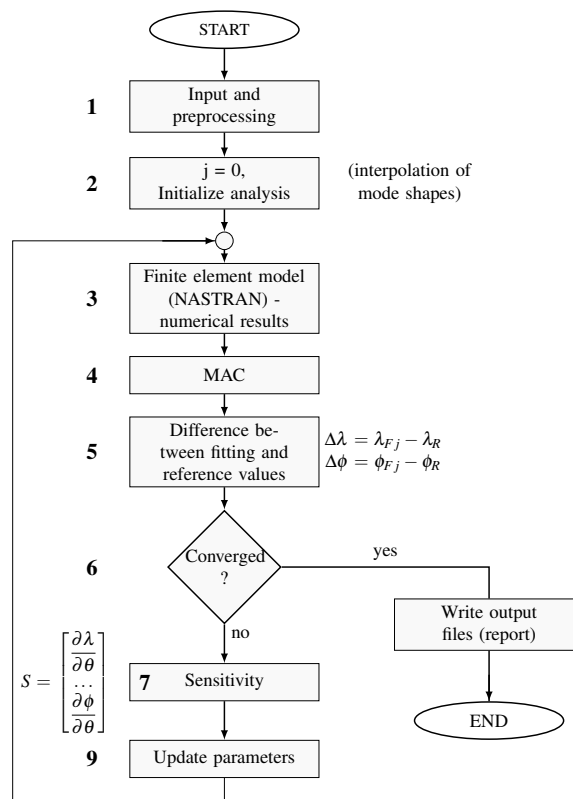


Figure 1: Parameters fitting method: algorithm flowchart.

In Fig. 1, steps 1 to 3 compute the solution of numerical FEM model with MSC Nastran™ solver. MAC in Step 4 is described in Sec. 2.2. At step 5 differences between numerical and actual eigenvalues and eigenvectors are calculated, these differences are used in step 6 where the convergence criterion is defined. If the modulus of $\Delta\lambda$ and $\Delta\phi$ are lower than an acceptable error, ϵ , fitting process is employed and the output files are written. However, if differences are bigger

than the error, fitting methodology is applied in blocks 7 to 9. Block 7 represents the sensitive matrix presented in Sec. 2.1, at block 8 the minimization process is calculated by Eq. 7 and at block 9 the adjusted parameters are obtained by Eq. 9. When differences become less than acceptable error the convergence is achieved.

4. NUMERICAL STUDIES

4.1 Isotropic beam

Following the study cases presented by Infantes (2000) where isotropic beams were analyzed, a similar configuration is studied here. The design variables θ_i are: θ_1 is the beam elasticity module, (E), θ_2 is the translational spring at the root (K_t), and θ_3 is the torsional spring at the root (K_r).

To begin the study, generic values were defined. For the chosen case, the density is not given by the cited reference (Infantes, 2000). Thus, a model close to that is defined, using a density that brings the frequencies close to the ones presented. It is interesting to note that the methodology can not be applied here because the mode shapes are not available.

In the present analysis, a coarser mesh model is used as reference and a finer mesh model is used as fitting model. This would be the condition where uncertainties related to experimental conditions are represented by the coarse mesh. To mention one of those experimental conditions, the number of available accelerometers or vibrometers is usually small, what leads to differences in the modal results. On the other hand, the numerical model can be further and further refined, until all desired modes are very well represented.

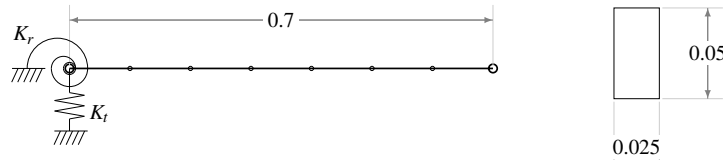


Figure 2: Isotropic beam model and dimensions.

Table 1: Design variables used in the reference model.

θ_i	Ref. values	Ref. frequencies (Hz)
1	E 61.0e9 Pa	1 f_1 39.69
2	$K_t x$ 50.0e6 N/m	2 f_2 244.83
3	K_r 100.0e3 N/m	3 f_3 668.04
	ρ 2100.0 kg/m^3	4 f_4 1262.22
		5 f_5 1988.88

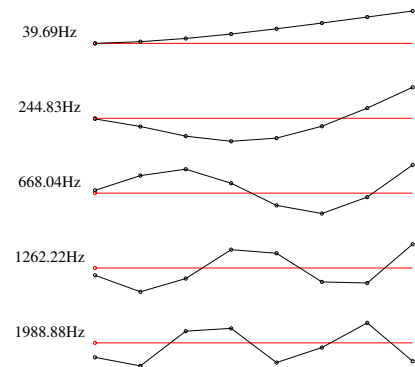


Figure 3: First 5 modes for the isotropic beam, modeled with 7 elements (8 nodes).

4.1.1 Reference and fitting models with 8 nodes

To verify the condition related to mode shapes interpolation, the same FE model is used both as input for the fitting model and as reference model. This situation does not require interpolation of modal displacements. Results are very good, both in frequencies and in mode shapes, as seen in Tab. 2 and Fig. 4.

Table 2: Fitted properties and frequencies for the isotropic beam model ($n_{modes} = 3$, $c_{conv} = 1e-5$.)

name	Reference	$\Delta\theta_i$	θ_0 (initial)	θ_{conv} (final)	Ref. freq.(Hz)	fitted freq. (Hz)	Error (%)
1	E 61.e9	0.01	30.0e9	61.00e9	f_1 39.69	39.6922	0.0055
2	K_x 50e6	0.05	10.0e6	49.99e6	f_2 244.83	244.8362	0.0025
3	K_α 100e3	0.05	10.0e3	99.99e3	f_3 668.04	668.0401	-0.0045
					f_4 1262.22	1262.221	0.0001

4.1.2 Reference model with 8 nodes and fitting model with 15 nodes

To simulate the case where interpolation is necessary, a refined model is used as fitting model. In the present case, it is necessary to interpolate the modes from the coarser reference model to the fitting model. The reference and interpolated mode shapes are shown in Fig. 5 for 5 modes. Analyzing the superimposed mode shapes by visual inspection, it is seen that up to the third mode there is a good representation, but after that, not so much. The MAC representation is not applied here because of the different number of nodes between both models.

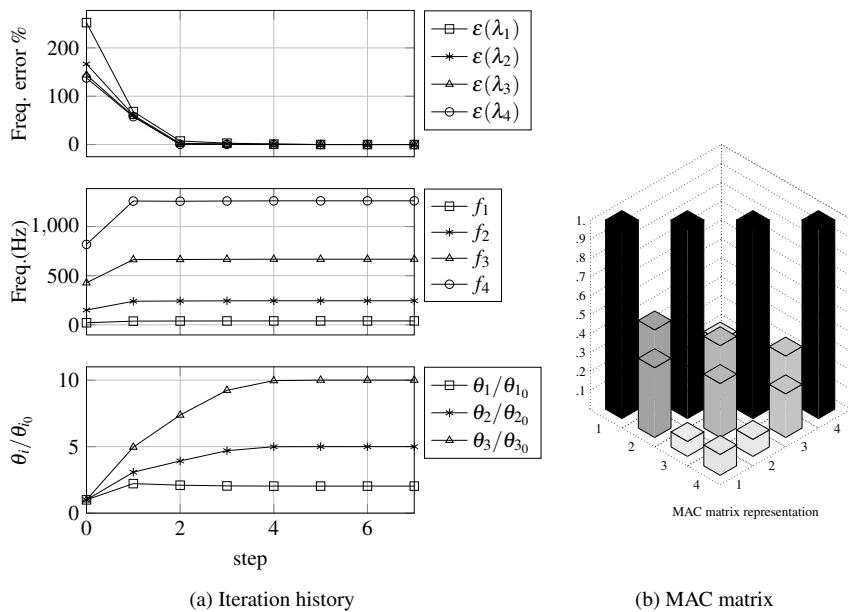


Figure 4: Iteration history fitting and MAC representation of the isotropic beam using 4 modes. Reference and fitting model with 8 nodes.

The first analysis considered three modes for fitting. Table 3 shows the resulting values for the fitted properties and Fig.6 has the iteration history and MAC graphic representation. It is noted that the torsional spring modeling is badly represented, but still the frequencies and mode shapes come to excellent agreement values.

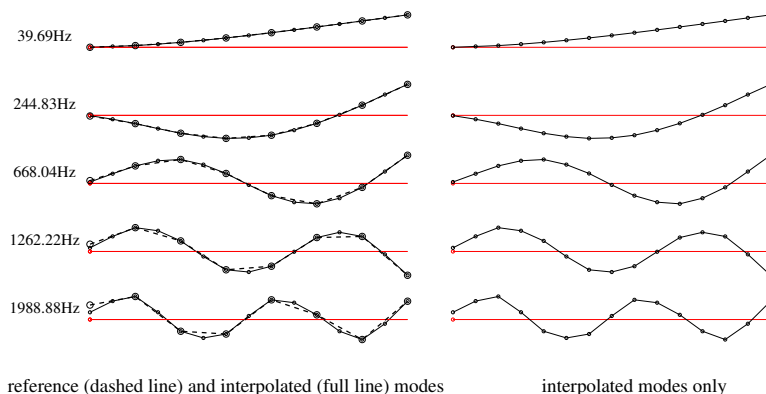


Figure 5: First 5 modes for the isotropic beam, modeled with 7 elements (8 nodes).

Table 3: Fitted properties and frequencies for the isotropic beam using interpolated models ($n_{modes} = 3$, $c_{conv} = 1e-5$).

name	Ref.	$\Delta\theta_i$	θ_0 (initial)	θ_{conv} (final)	Ref. freq.(Hz)	fitted freq. (Hz)	Error (%)		
1	E	61.e9	0.01	30.0e9	52.84e9	f_1	39.69	39.69220	0.0055
2	K_x	50e6	0.05	10.e6	43.27e6	f_2	244.83	244.8362	0.0025
3	K_α	100e3	0.05	10.e3	256.26e3	f_3	668.04	668.0400	0.0000

4.2 Generic composite flat plate

To apply the methodology to an orthotropic plate, a model with the same dimensions of those described by [de Souza et al. \(2013\)](#) is used. Here, the properties of a glass-epoxy (Gl.-Ep.) fabric (as given by [Reddy \(1997\)](#)) are considered, with a density of 1900 kg/m^3 . Detailed properties values are given in Tab. 4.

This is a simplified composite model, since it has only one layer of thickness of 2mm, with a single orientation θ_k for the whole model. However, three different variations are simulated: $\theta_k = 0^\circ$, 45° and 90° . The model is seen in Fig. 7, where the reference angle for the material orientation is given. Modal shape results are presented in Fig. 8, where the influence of the orientation θ_k is easily observed. First, there is a mode crossing between the second and third modes, where the first torsion changes place with the second bending form 0° to 90° . In the middle, the second and third modes present a mixed behavior, for $\theta_k = 45^\circ$.

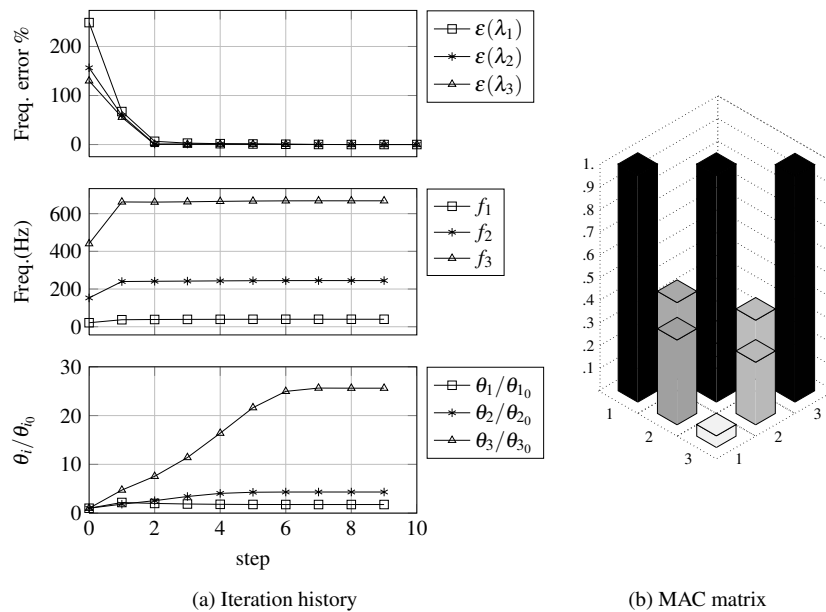
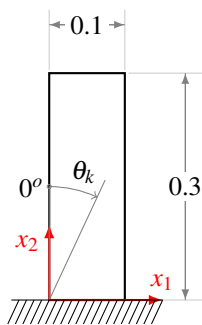
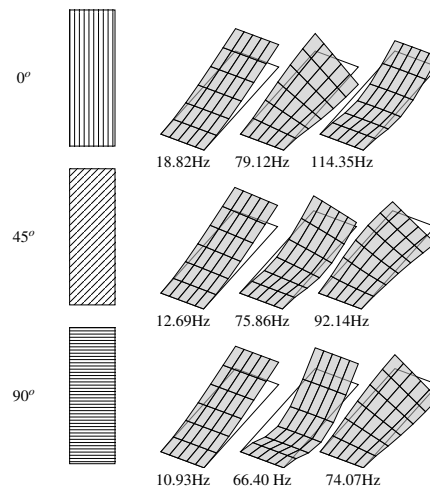


Figure 6: Results for a run of the isotropic beam using 3 modes. Reference model: 8 nodes. Fitting model: 15 nodes .

Table 4: Design variable values used in the reference model for the orthotropic plate made of GI-Ep.

θ_i	Reference value	Reference frequencies (Hz)					
1	E_1	53.0e9	Pa	f_1	$\theta_k = 0^\circ$	$\theta_k = 45^\circ$	$\theta_k = 90^\circ$
1	E_2	17.9e9	Pa	f_2	18.82	12.69	10.93
1	G_{12}	8.9e9	Pa	f_3	79.12	75.86	66.40
2	ν_{12}	0.25	N/m	f_4	114.35	92.14	74.07
	ρ	1900.0	kg/m^3		253.16	209.84	181.31
	e_t	2e-3	m				

Figure 7: Composite flat plate model dimensions showing the lamina reference angle. The global coordinates follow the aviation practice, where x_1 points to the wind direction and x_2 is parallel to the wing.Figure 8: First 3 modes for orthotropic plate, for $\theta_k = 0^\circ, 45^\circ$ and 90° .

Only these three modes will be considered in the analysis in the present work. The fourth mode frequency is listed in Tab. 4 to show the distance to the third one. For aeroelastic purposes, it is expected that this mode will not present a large influence on stability or LCO results.

The reference FE model is composed of 42 nodes and 30 quadrilateral elements (CQUAD4). The first analysis consists in adjusting this model, where the reference model has the specified properties and the fitting model is setup with lower arbitrary tentative values. The design variables are the lamina engineering properties E_1 , E_2 and G_{12} .

In the case of orthotropic plates, the lamina orientation plays an important role. Here, θ_k is initially set to 0° . The convergence is very fast, when using only three modes. However, from Tab. 5 it is noticed that not all variables were correctly fitted, and the value of E_2 obtained was way above the reference value. Analyzing the model and mode shapes

on Fig. 8, it is observed that for $\theta_k = 0^\circ$, E_2 is not very significant for the modes behavior, and the modal response is governed more by the E_1 and G_{12} contributions to the bending and torsion modes encountered.

Now applying the fitting process to the plate with θ_k is initially set to 45° , the response is closer for all design variables, but still not ideal. In this case, the second and third modes present a mixed behavior, where all the three engineering parameters participate in a certain amount. The fitted frequencies, on the other side, show an excellent agreement with the reference one, as well as the mode shapes, as indicated by the MAC matrix representations on Fig. 10.

Finally, when applying the fitting process to the plate with θ_k is initially set to 90° , the response is very good for E_2 and G_{12} , but not for E_1 , as seen on Tab. 7. This is also related to the influence of E_1 on the first three mode shapes that were taken as reference for the fitting process.

Here, it is necessary to recall the goal of the fitting parameters process in the aeroelastic analysis area: obtain parameters for the numerical model so that it represents adequately the modal behavior of the physical model.

Table 5: Fitted properties for the Gl.-Ep. model ($n_{modes} = 3, c_{conv} = 1e-5.$) - $\theta_k = 0^\circ$

name	Ref.	$\Delta\theta_i$	θ_0 (initial)	θ_{conv} (final)	Ref. freq. (Hz)	Fitted freq. (Hz)	Error (%)		
1	E_1	53.0e9	0.01	10.0e9	52.53e9	f_1	18.82	18.82	0.000
2	E_2	17.9e9	0.05	5.e9	37.91e9	f_2	79.12	79.12	0.000
3	G_{12}	8.9e9	0.05	1.e9	8.86e9	f_3	114.35	114.35	0.000

Table 6: Fitted properties for the Gl.Ep. model ($n_{modes} = 3, c_{conv} = 1e-5.$) - $\theta_k = 45^\circ$

name	Ref.	$\Delta\theta_i$	θ_0 (initial)	θ_{conv} (final)	Ref. freq. (Hz)	Fitted freq. (Hz)	Error (%)		
1	E_1	53.0e9	0.01	10.0e9	54.23e9	f_1	12.69	12.83	1.1032
2	E_2	17.9e9	0.05	5.e9	16.06	f_2	75.86	75.86	0.0000
3	G_{12}	8.9e9	0.05	1.e9	10.14e9	f_3	92.14	92.14	0.0000

Table 7: Fitted properties for the Gl.-Ep. model ($n_{modes} = 3, c_{conv} = 1e-5.$) - $\theta_k = 90^\circ$

name	Ref.	$\Delta\theta_i$	θ_0 (initial)	θ_{conv} (final)	Ref. freq. (Hz)	Fitted freq. (Hz)	Error (%)		
1	E_1	53.0e9	0.01	10.0e9	13.29e9	f_1	10.93	10.94	0.0915
2	E_2	17.9e9	0.05	5.e9	17.63	f_2	66.40	66.40	0.0000
3	G_{12}	8.9e9	0.05	1.e9	8.88e9	f_3	74.07	74.07	0.0000

4.2.1 Study of interpolated models

To continue the verification of the methodology, it is necessary to test reference and fitting models with a different number of nodes, what makes necessary to perform an interpolation process prior to the fitting process. A FE model with 63 nodes and 48 quadrilateral elements is used as fitting model for this case. The analysis follows a similar procedure as in the described above, where the fitting is performed for different orientations.

First, the model with $\theta_k = 0^\circ$ is analyzed with the same initial values used in the above cases, considering that there is no knowledge about the actual values. From Tab. 8 and Fig. 11 it is observed that the same behavior of previous analyzes: the E_2 result for the first run is not close to the reference value, despite the frequencies and MAC results being adequate.

From the results of the first run, new initial values are used for $\theta_k = 90^\circ$, as seen on Tab. 9. These values are very close to the fitted values given in Tab. 8. Now, the values for all three variables are very close to the reference ones. Frequencies and mode shapes results are very good.

Table 8: Fitted properties for the interpolated Gl.-Ep. model ($n_{modes} = 3, c_{conv} = 1e-5.$) - $\theta_k = 0^\circ$

name	Ref.	$\Delta\theta_i$	θ_0 (initial)	θ_{conv} (final)	Ref. freq. (Hz)	Fitted freq. (Hz)	Error (%)		
1	E_1	53.0e9	0.01	10.0e9	52.29e9	f_1	18.82	18.57	-1.3284
2	E_2	17.9e9	0.05	5.e9	7.66e9	f_2	79.12	79.12	0.0000
3	G_{12}	8.9e9	0.05	1.e9	9.09e9	f_3	114.35	114.35	0.0000

Table 9: Fitted properties for the interpolated Gl.-Ep. model ($n_{modes} = 3, c_{conv} = 1e-5.$) - $\theta_k = 90^\circ$

name	Ref.	$\Delta\theta_i$	θ_0 (initial)	θ_{conv} (final)	Ref. freq. (Hz)	Fitted freq. (Hz)	Error (%)		
1	E_1	53.0e9	0.01	50.0e9	50.83e9	f_1	10.93	10.78	-1.3724
2	E_2	17.9e9	0.05	7.e9	17.42e9	f_2	66.40	66.40	0.0000
3	G_{12}	8.9e9	0.05	8.e9	8.80e9	f_3	74.07	74.07	0.0000

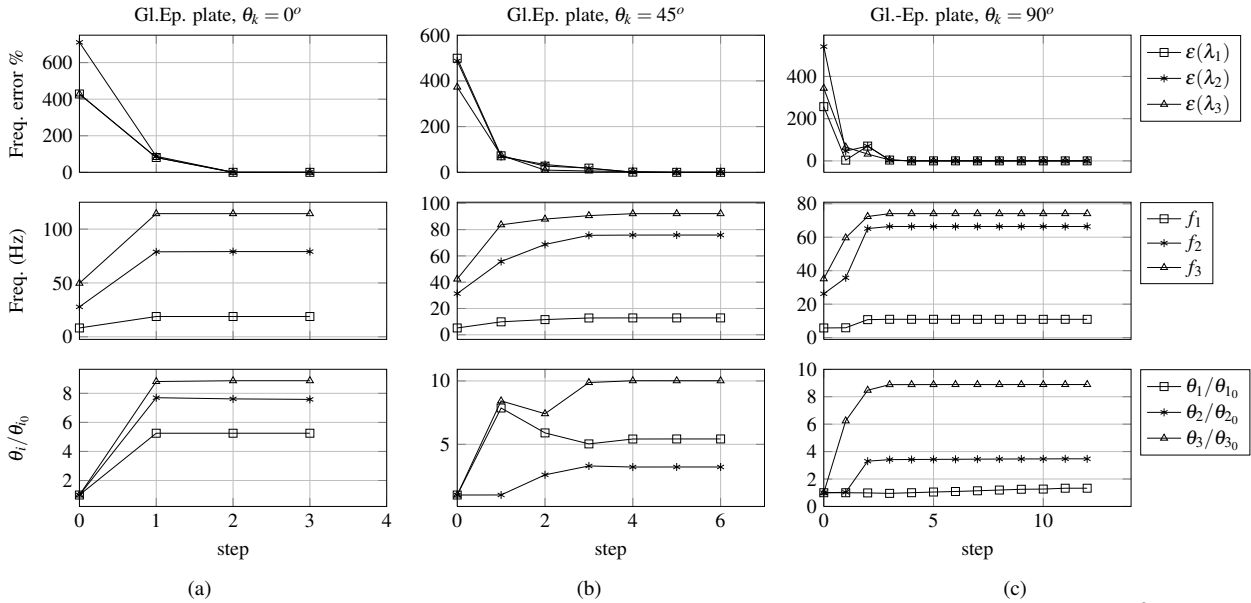


Figure 9: Convergence history for the Gl.Ep. model, considering three modes. On the left, results for $\theta_k = 0^\circ$ and on the right for $\theta_k = 90^\circ$.

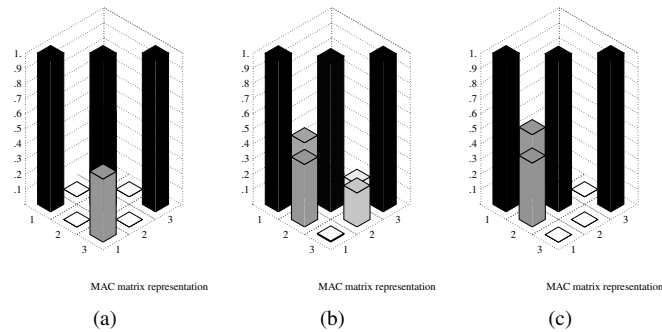


Figure 10: MAC matrix representation for Gl.Ep. model with $\theta_k = 0^\circ, 45^\circ$ and 90° .

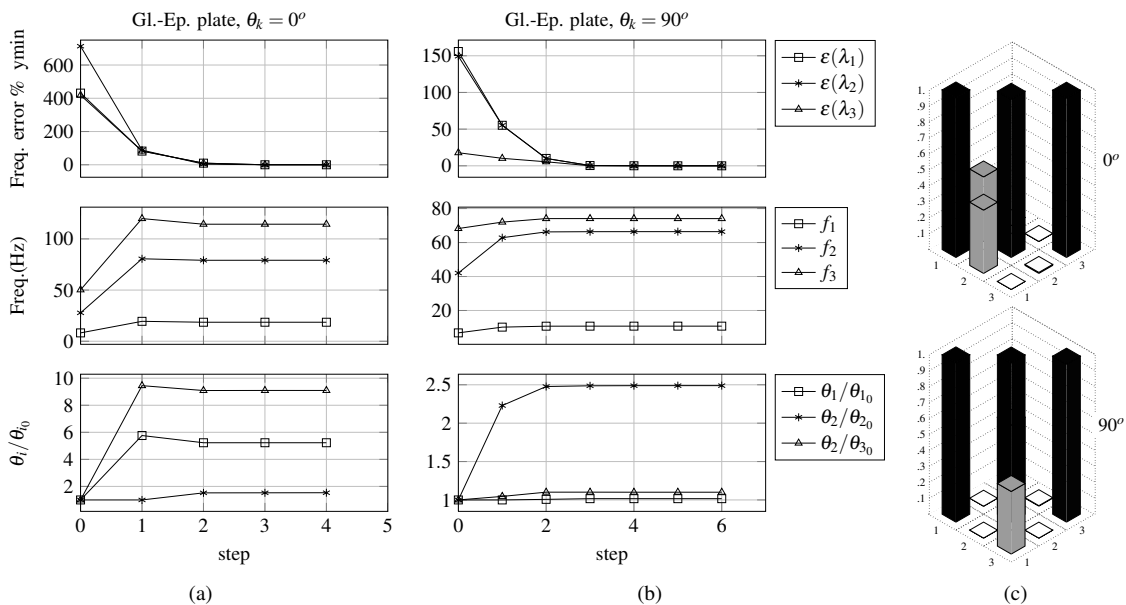


Figure 11: Convergence history for the interpolated Gl.Ep. model, considering three modes. On the left, results for $\theta_k = 0^\circ$ and on the right for $\theta_k = 90^\circ$.

4.3 Carbon fiber flat plate - comparison with experiment

The present methodology is applied to the numerical model fitting using the experimental results described in [de Souza et al. \(2013\)](#). In that work, composite flat plates designed for aeroelastic studies were characterized aiming definition of modal parameters for aeroelastic purposes. The geometric model is the same of Fig. 7, but the material here is carbon fiber and epoxy matrix. Also, the thickness of the models are only 1.5mm. A total of five plates were considered. From the total mass of the plates and their volume, it was possible to compute the density, that is 1427 kg/m^3 .

A first run was performed with $\theta_k = 0^\circ$, and the results are shown in Tab. 10 and Fig. 12 (a). Again, results are very good for frequency values and mode shapes. Since now there is no information about the engineering parameters of the experimental models, it is not possible to compare values.

Considering that the obtained parameters are good, they are rounded off to serve as input values for the analysis of $\theta_k = 90^\circ$, as seen on Tab. 11. A fast convergence is obtained in this case also, and values are very close to the previous one. As in the other cases, frequencies and mode shapes match with reference values.

To complete the study, the obtained parameters were used in the FE model to obtain frequencies and mode shapes for the 5 different orientations described by [de Souza et al. \(2013\)](#). From the first case, is taken as $E_1 = 92.7 \text{ GPa}$. From the second case, E_2 is made 6.7 GPa . The in-plane shear module G_{12} is taken as an average between both cases, i.e., 4.35 GPa . The resulting frequencies and mode shapes match the experimental results, as seen on Fig. 13.

Table 10: Fitted properties for the experimental model ($n_{modes} = 3, c_{conv} = 1e-5$) - $\theta_k = 0^\circ$

name	$\Delta\theta_i$	$\theta_0(\text{initial})$	$\theta_{conv}(\text{final})$	Ref. freq.(Hz)	Fitted freq.(Hz)	Error (%)		
1	E_1	0.05	30.0e9	92.71e9	f_1	20.8	21.44	3.0769
2	E_2	0.05	5.e9	4.39e9	f_2	53.12	53.12	0.0000
3	G_{12}	0.05	1.e9	4.09e9	f_3	130.37	130.36	-0.0077

Table 11: Fitted properties for the experimental model ($n_{modes} = 3, c_{conv} = 1e-4$) - $\theta_k = 90^\circ$

name	$\Delta\theta_i$	$\theta_0(\text{initial})$	$\theta_{conv}(\text{final})$	Ref. freq.(Hz)	Fitted freq.(Hz)	Error (%)		
1	E_1	0.01	90.0e9	86.82e9	f_1	5.7	5.79	1.5789
2	E_2	0.05	5.e9	6.76e9	f_2	35.25	35.22	-0.0851
3	G_{12}	0.05	4.e9	4.68e9	f_3	45.87	45.80	-0.1526

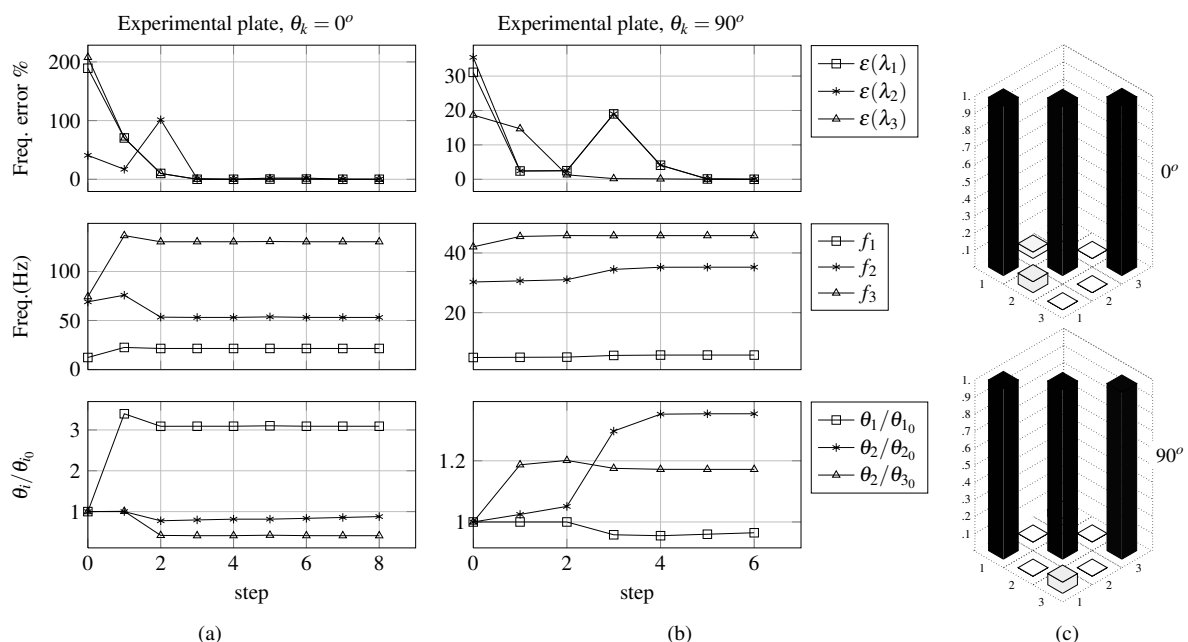


Figure 12: Convergence history for the experimental model, considering 3 modes. On the left, results for $\theta_k = 0^\circ$ and on the right for $\theta_k = 90^\circ$.

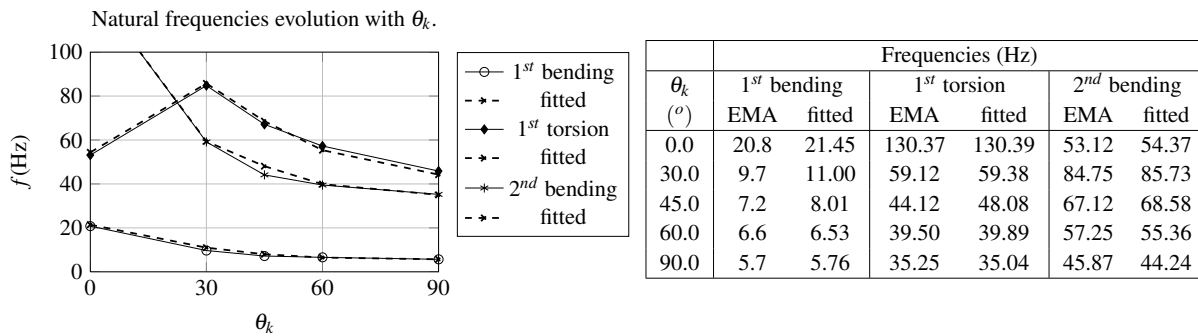


Figure 13: Frequencies obtained with fitted numerical models compared to experimental values.

5. CONCLUDING REMARKS

This paper discussed the modal parameters fitting of composite flat plates. These plates are intended for use in aeroelastic analysis, where a numerical model with adequately adjusted frequencies and mode shapes is employed in the structural side of the problem. The method has been implemented numerically, coupling MSC NastranTM and MatlabTM.

The sensitivities are calculated by finite differences, what showed to be efficient for the present work purposes. The application of interpolation methods is necessary to bring the reference mode shapes to the studied model. This process has to be done with special attention because modes not adequately represented by the experiments, when included in the fitting process, can affect the results.

The next steps include a few tasks to improve the present methodology. It is shown to be necessary a refinement of the interpolation procedures, to transmit also the boundary conditions. Also, when applying the methodology to composite plates, made of orthotropic material, the condition where the sensitivity to certain design variable is very low can lead to instabilities in the fitting process. This effect needs to be addressed. To complete the tests, it is necessary to apply the same equivalent springs to the plate models, trying to represent the experimental boundary conditions.

For aeroelastic purposes the goal is to have the same modal response, and the results expected is to have adequately fitted frequencies and associated mode shapes. The methodology as implemented in the present work satisfies this goal, and is already being employed in aeroelastic analyses.

6. ACKNOWLEDGEMENTS

The second author acknowledges the partial support from the Instituto Nacional de Ciência e Tecnologia - Estruturas Inteligentes em Engenharia, INCT-EIE.

7. REFERENCES

- Allemang, R.J., 2003. "The modal assurance criterion—twenty years of use and abuse". *Sound and Vibration*, Vol. 37, No. 8, pp. 14–23.
- Carneiro, S.H.S., 1993. *Ajuste do modelo dinâmico de sistemas multicorpos flexíveis*. Master's thesis, Instituto Tecnológico de Aeronáutica, São José dos Campos.
- de Souza, C.E., Marto, A.G., da Silva, R.G.A., Inojosa, L.A. and Oliveira, E.L., 2013. "Characterization of flexible composite wings through experimental and operational modal analyses". In M.A. Savi, ed., *Proceedings of the XV International Symposium on Dynamic Problems of Mechanis*. Búzios, Brasil.
- Göge, D., 2003. "Automatic updating of large aircraft models using experimental data from ground vibration testing". *Aerospace science and technology*, Vol. 7, No. 1, pp. 33–45.
- Infantes, J.E.C., 2000. *Ajuste de Modelos de Elementos Finitos Usando Técnicas de Estimação de Parâmetros*. Master's thesis, Universidade Estadual de Campinas.
- Jurado, J., Hernandez, S. and Nieto, F., 2012. *Bridge Aeroelasticity: Sensitivity Analysis and Optimum Design*. WIT Press.
- Lahey, R.S., ed., 1983. *Design Sensitivity in MSC/NASTRAN*. Nastran User's Conference Proceedings.
- Reddy, J., 1997. *Mechanics of Laminated Composite Plates: theory and analysis*. CRC Press, Boca Raton, FL.
- ZONA Technology, ed., 2007. *ZAERO Theoretical Manual*. Version 8.0. ZONA Tech.

8. RESPONSIBILITY NOTICE

The authors are the only responsible for the printed material included in this paper.